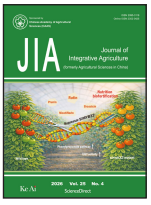
Journal of Integrative Agriculture 2026, 25(4): 1531–1543

KeAi
CHINESE ROOTS
GLOBAL IMPACT

Available online at ScienceDirect

Journal of Integrative Agriculture



RESEARCH ARTICLE

Cloning and functional characterization of *LiDXR* gene from Oriental Lily (*Lilium* 'Sorbonne')

Xinyue Zhang, Jingqi Dai, Fan Jiang, Tao Yang, Jinzhu Zhang, Jie Dong, Jinping Fan#

College of Horticulture & Landscape Architecture, Northeast Agricultural University, Harbin 150030, China

Highlights

- Virus-induced gene silencing (VIGS)-mediated suppression of *LiDXR* specifically downregulated monoterpenoid synthase genes TPS1/3/4, without affecting the sesquiterpenoid synthase TPS2, revealing a selective regulatory mechanism in lily floral scent biosynthesis.
- LiDXR functions as a key rate-limiting enzyme in the methylerythritol phosphate (MEP) pathway, with peak expression in petals at the semi-open floral stage, aligning with the temporal dynamics of terpenoid emission in lily.

Abstract

Floral scent is an important ornamental trait in garden plants. Monoterpenes, a major class of terpenoids, constitute the primary volatile components of lily floral scents. 1-Deoxy-D-xylulose 5-phosphate reductoisomerase (DXR) catalyzes the second enzymatic step in the MEP pathway, which supplies precursors for monoterpene biosynthesis. However, the functional role of the *DXR* gene in floral monoterpene production in *Lilium* Oriental Hybrid 'Sorbonne' remains unclear. In this study, 'Sorbonne' was used as the experimental material, and a differentially expressed *LiDXR* gene was identified from early transcriptomic data, showing high temporal correlation with the synthesis and emission dynamics of floral volatiles during flowering. The *LiDXR* gene was cloned and subjected to bioinformatics analysis, revealing that it encodes a protein of 472 amino acids. *LiDXR* expression peaked at the half-open floral stage and was significantly higher in petals than in other floral organs. Subcellular localization analysis indicated that the LiDXR protein is targeted to chloroplasts in leaf epidermal cells. VIGS of *LiDXR* reduced monoterpene levels by downregulating the expression of downstream *TPS* genes in the MEP pathway. Consistently, headspace solid-phase microextraction coupled with gas chromatography-mass spectrometry (HS-SPME-GC-MS) revealed a significant decrease in total volatile terpene content in silenced lilies. Transgenic *Arabidopsis thaliana* and petunia plants overexpressing *LiDXR* exhibited enhanced growth vigor and accelerated flowering. GC-Murashige and Skoog's (MS) analysis of transgenic petunias showed a 78% increase in total volatile terpenes compared to wild-type plants. Overexpression of *LiDXR* also modulated the expression of other MEP pathway genes, thereby influencing the biosynthesis of downstream terpenoids, including monoterpenes. This study elucidates the functional role of *LiDXR* in terpenoid metabolism and provides a theoretical foundation for floral scent breeding in lily and other ornamental plants.

Keywords: *Lilium*, floral, monoterpene, *LiDXR*

1. Introduction

Due to their sessile nature, plants must continuously adapt to environmental fluctuations to ensure survival and reproductive success. In response to these dynamic conditions, plants have evolved a diverse array of metabolites, commonly referred to as plant secondary metabolites or plant natural products (Muhlemann *et al.* 2014). Among these, floral volatiles represent a class of lipophilic compounds characterized by low molecular weight and high vapor pressure at ambient temperatures. These physical properties enable them to diffuse freely across cell membranes and be released into the surrounding environment (Pichersky *et al.* 2006). Based

Received 14 September 2024; Received in revised form 14 January 2025; Accepted 8 April 2025; Available online 7 November 2025
Xinyue Zhang, E-mail: 13734523745@163.com; #Correspondence Jinping Fan, E-mail: jinpingfan@neau.edu.cn

© 2026 CAAS. Publishing services by Elsevier B.V. on behalf of KeAi Communications Co. Ltd. This is an open access article under the CC BY-NC-ND license (http://creativecommons.org/licenses/by-nc-nd/4.0/). Peer review under responsibility of Editorial Board of *Journal of Integrative Agriculture*.
doi: 10.1016/j.jia.2025.11.002

on their biosynthetic origins, floral volatiles are broadly classified into three categories: terpenoids, phenylpropanoids/benzenoids, and fatty acid derivatives. Terpenoids constitute the most abundant class of plant natural products, with the number of identified structures doubling approximately every decade since the 1970s. These compounds fulfill diverse functional roles in plants, including acting as hormones (e.g., gibberellins, abscisic acid), photosynthetic pigments (e.g., carotenoids), and electron carriers in respiratory and photosynthetic chains. Terpenoids also serve as precursors to plastoquinone, ubiquinone, polyprenyl phosphates involved in protein glycosylation, and membrane components such as phytosterols (Opitz *et al*. 2014). As the largest group of volatile organic compounds (VOCs), terpenoids are biosynthesized *via* two distinct pathways: The cytosolic mevalonate (MVA) pathway produces sesquiterpenes and triterpenes, whereas the plastidial methylerythritol phosphate (MEP) pathway mediates the formation of monoterpenes, diterpenes, and carotenoids (Tholl *et al.* 2005). Both the MEP and MVA pathways generate the fundamental C5 isoprene units required for terpene biosynthesis, with key transformations catalyzed by enzymes belonging to the terpene synthase (TPS) family. Members of the TPS family determine the carbon skeleton, ring number, and stereochemistry of terpenes through the formation of specific terpene backbones, which are subsequently modified by enzymatic reactions such as methylation, demethylation, and isomerization.

As research into the functional role of the MEP pathway in terpene biosynthesis has advanced, aided by developments in molecular biotechnology and high-throughput sequencing, numerous studies have focused on isolating and characterizing the key enzymes and their encoding genes within this pathway. These efforts have identified 1-deoxy-D-xylulose 5-phosphate synthase (DXS) and 1-deoxy-D-xylulose 5-phosphate reductoisomerase (DXR) as potential rate-limiting enzymes. Overexpression of *GrDXR* in geranium has been shown to increase the yield of secondary metabolites, particularly geranium essential oil (Jadaun *et al.* 2017). In transgenic peppermint plants overexpressing DXR, enzyme activity increased 24-fold, accompanied by a 50% increase in leaf volatile oil content (Mahmoud and Croteau 2001). Conversely, loss-of-function mutations in DXR in *Arabidopsis thaliana* result in albinism, severe dwarfing, and eventual lethality (Xing *et al.* 2010). Collectively, these findings underscore the critical role of DXR in regulating carbon flux through the MEP pathway. Although DXS catalyzes the first committed step of the MEP pathway, its product, DXP, serves as a metabolic branch point, functioning not only as a precursor to isoprenoids but also to essential cofactors such as thiamine pyrophosphate (TPP) and pyridoxal phosphate (Carretero-Paulet *et al.* 2002). Given this dual metabolic role, the DXR-catalyzed conversion of DXP to MEP may represent the first dedicated step toward plastidial isoprenoid biosynthesis, positioning DXR as a key regulatory node in the production of terpenoid volatiles (Fig. 1). Despite these advances, the identification

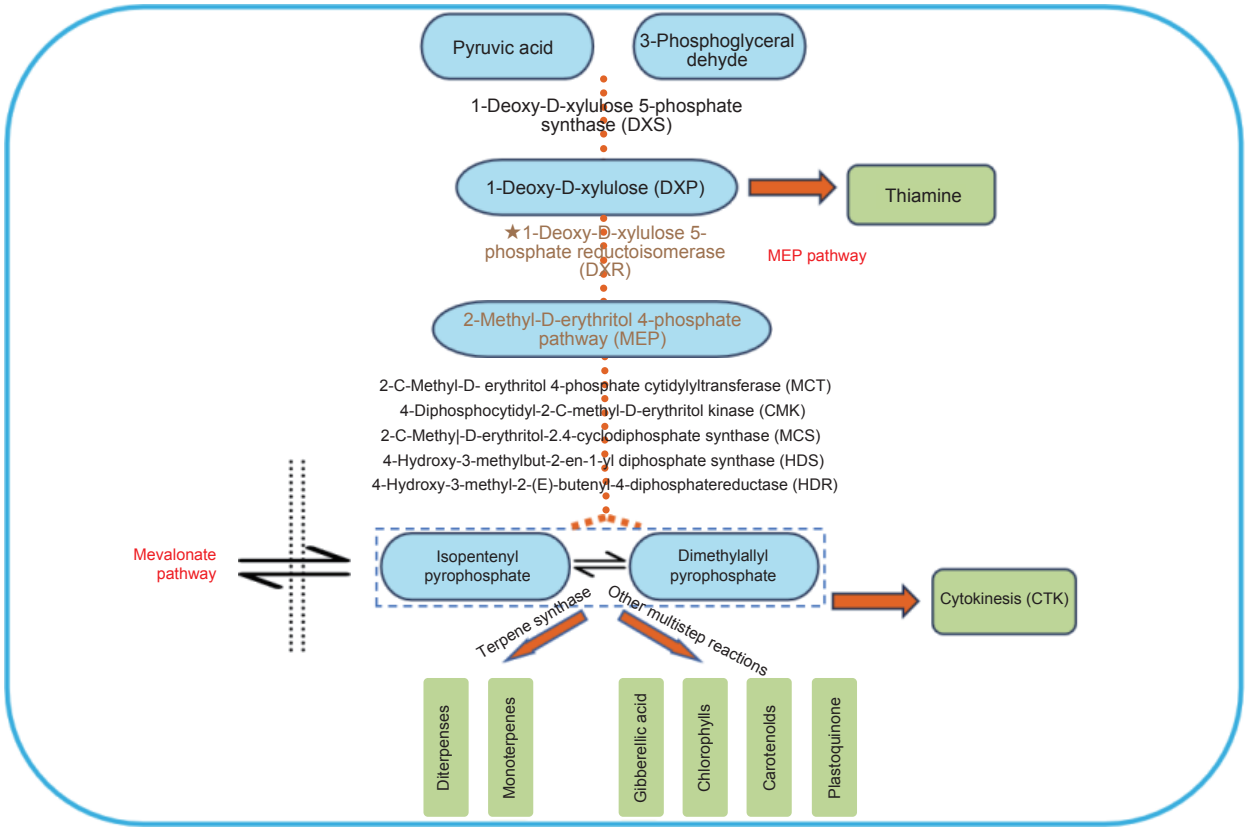


Fig. 1 Specific location of DXR enzyme in methylerythritol phosphate (MEP) pathway.

and functional characterization of rate-limiting genes in the MEP pathway in lily, as well as their specific regulatory roles in floral scent biosynthesis, remain poorly understood.

To investigate the function of the *DXR* gene in plant terpenoid biosynthesis, the *DXR* gene has been cloned and characterized in numerous plant species. It has been found that the *DXR* gene typically exists as a single copy in the plant genome and exhibits differential expression across various plant tissues. Currently, studies on the *DXR* gene are widespread in ornamental plants such as orchids, chrysanthemums, and periwinkle, as well as in medicinal plants including *Rehmannia*, *Tripterygium*, and *Petasites*. Related research has also been reported in tree species such as *Taxus chinensis*, *Ginkgo biloba*, and *Fructus chinensis*. The tissue-specific expression patterns of the *DXR* gene generally align with the accumulation profiles of terpenoids. Camptothecin, a significant terpenoid compound produced by *Camptotheca acuminata*, is widely used as an anticancer agent and is primarily stored in the bark and branches. Tissue expression analysis of the *CaDXR* gene in *Camptotheca* revealed strong expression in stems and weak expression in leaves and roots, consistent with the primary sites of camptothecin accumulation (Yao *et al.* 2008). A similar pattern was observed in rose-scented *Pelargonium* spp., where leaves are rich in aromatic terpene essential oils with important applications in the chemical and food industries. In comparison to stem, petiole, and root tissues, *GrDXR* showed significantly higher expression levels in leaves (Jadaun *et al.* 2017). In addition to spatial differences, *DXR* gene expression also displays temporal regulation, with distinct expression dynamics across different stages of the plant life cycle. In *Artemisia apiacea*, expression profiling of artemisinin and its biosynthetic pathway genes — across three developmental stages: leaf expansion, pre-flowering, and post-flowering — revealed that *AaDXR* expression was lowest during leaf expansion, gradually increased, and peaked just before flowering. Following flowering, *AaDXR* expression declined. The roots and leaves of *Withania somnifera* (L.) Dunal are rich in bioactive withanolides, particularly solanolactone. Studies on the expression of the key biosynthetic gene *WsDXR* at different growth stages showed that its expression level during the reproductive growth stage was 2.24-fold higher than during the vegetative growth stage (Orru *et al.* 2023).

These results suggest that the *DXR* gene plays a critical role in the MEP pathway and contributes significantly to the synthesis and accumulation of plant terpenoids. However, the specific regulatory effect of the *DXR* gene on floral monoterpenes — key downstream products of the MEP pathway — remains unclear. In lily, petals are the primary site for the release of volatile compounds (Johnson *et al.* 2016). Compared with non-aromatic *Lilium* species, aromatic *Lilium* varieties are characterized by higher levels of monoterpenoids and benzenoids, particularly monoterpenes such as myrcene, linalool, and 1,8-cineole, as well as methyl benzoate (Kong *et al.* 2012). Therefore, elucidating the precise function of the *DXR* gene in the MEP pathway is essential for understanding the biosynthesis and regulatory mechanisms of floral volatiles in lily.

2. Materials and methods

2.1. Plant materials and growth conditions

The plant materials used in this study include *Lilium* Oriental Hybrid 'Sorbonne', *Nicotiana benthamiana* seeds, *Petunia hybrida* W115 seeds, and *A. thaliana* wild-type (Col-0) seeds, all preserved by the Garden Plant Breeding Laboratory of Northeast Agricultural University, China. *Arabidopsis thaliana dxr* mutant (SAIL-621-C03) seeds were obtained from the AraShare germbank (https://www.arashare.cn/index/). All plant materials were cultivated in the Garden Plant Genetics and Breeding Laboratory of Northeast Agricultural University under controlled environmental conditions: a 12/12 h (light/dark) photoperiod during the vegetative growth phase and 14/10 h during the reproductive phase, 40–60% relative humidity, and a temperature range of 22–24°C.

2.2. Transcriptome DEGs screening

Based on previously generated (unpublished) transcriptome sequencing data of 'Sorbonne' across five flower developmental stages — green bud, pink bud, half-open, blooming, and decay stages (Fig. 2-A) — combined with KEGG pathway analysis of terpenoid biosynthesis and prior research experience, 27 unigenes annotated to the MEP pathway were identified. Following BLAST comparison and removal of redundant gene sequences, seven representative MEP pathway genes were selected. Using expression data from 15 samples (three biological replicates across five stages) and RPKM values, principal component analysis (PCA) and cluster heat map analyses were performed to identify key candidate genes potentially regulating the MEP pathway.

2.3. RNA extraction and gene cloning

Total RNA was extracted from 80–100 mg of petal tissue of 'Sorbonne' at each of the five developmental stages using the TransZol Plant Kit (TransGen Biotech, Beijing, China), following the manufacturer's protocol for polysaccharide- and polyphenol-rich plant tissues. RNA quality was assessed using an ultra-micro ultraviolet spectrophotometer, and RNA integrity was confirmed by 1.2% agarose gel electrophoresis. First-strand cDNA was synthesized from 1 μg of total RNA using the *EasyScript*® Reverse Transcription System (TransGen Biotech, Beijing, China). Gene-specific primers were designed based on the open reading frame (ORF) identified in RNA-Seq data to amplify the full-length *LiDXR* sequence *via* PCR. All primers used in this study are listed in Appendix A.

2.4. Bioinformatics analysis

DNAman 9.0 was used to align the nucleotide and amino acid sequences of *LiDXR*. Subcellular localization of the LiDXR protein was predicted using WoLF PSORT (https://www.genscript.com/wolf-psort.html), ChloroP 1.1 server (http://www.cbs.dtu.dk/services/ChloroP/), and TargetP-2.0 server (http://www.cbs.dtu.dk/services/TargetP/) were used to predict the subcellular localization of LiDXR protein.

NCBI (https://www.ncbi.nlm.nih.gov/) was used to analyze the conserved domains of the LiDXR amino acid sequence, and Blastp was employed to assess sequence homology.

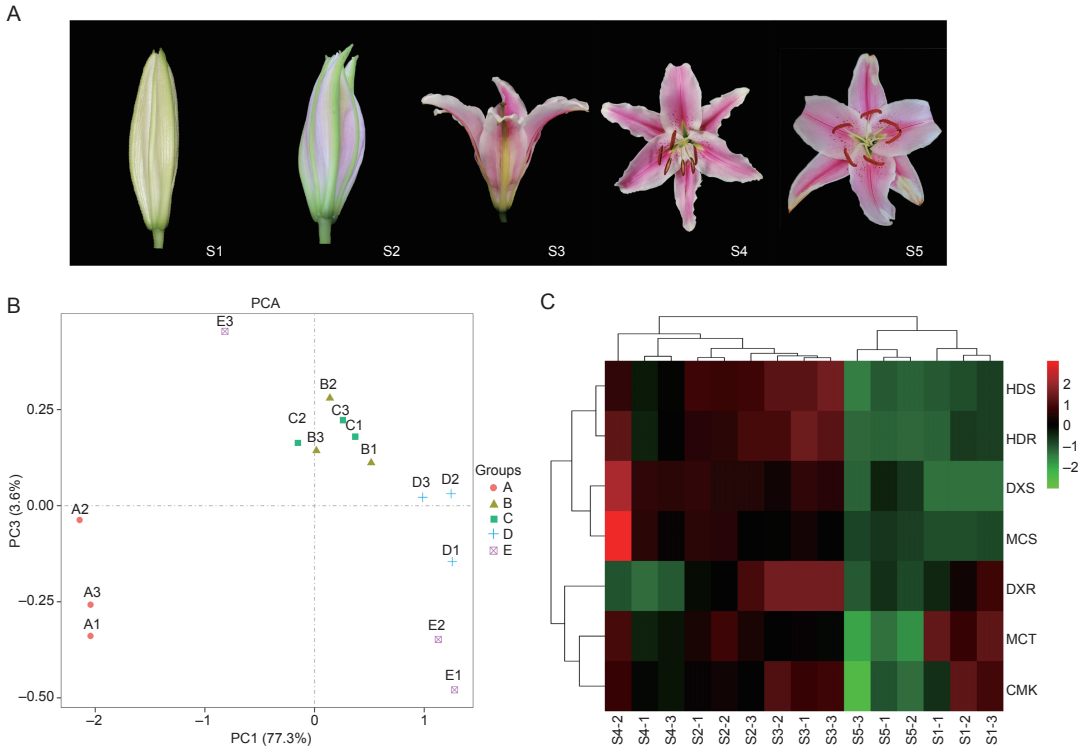


Fig. 2 *LiDXR* gene expression profiling across developmental stages. A, five flowering stages of 'Sorbonne'. B, PCA analysis of methylerythritol phosphate (MEP) pathway gene expression at different stages. C, hierarchical clustering heatmap of MEP pathway gene expression. S1, A, green bud stage; S2, B, pink bud stage; S3, C, half-open stage; S4, D, blooming stage; S5, E, senescence stage. HDS, 4-hydroxy-3-methylbut-2-enyl diphosphate synthase; HDR, 4-hydroxy-3-methylbut-2-enyl diphosphate reductase; DXS, 1-deoxy-D-xylulose 5-phosphate synthase; DXR, 1-deoxy-D-xylulose 5-phosphate reductoisomerase; MCT, 2-C-methyl-D-erythritol 4-phosphate cytidylyltransferase; CMK, 4-diphosphocytidyl-2-C-methyl-D-erythritol kinase; MCS, 2-C-methyl-D-erythritol 2,4-cyclodiphosphate synthase.

Phylogenetic analysis of the LiDXR protein was conducted using MEGA-X, with the evolutionary tree constructed *via* the neighbor-joining method and 1,000 bootstrap replications. The resulting phylogenetic tree was visualized and refined using EvolView (https://evolgenius.info//evolview-v2/#login).

2.5. Analysis of expression patterns of *LiDXR* gene

To verify the spatial expression pattern of the *LiDXR* gene in lily flowers and its expression dynamics during flower development, qRT-PCR was performed to determine the relative expression levels in different floral organs (sepals, filaments, anthers, petals) and leaves during the semi-blooming stage of 'Sorbonne'. Based on organ-specific expression profiles, petals from five developmental stages of 'Sorbonne' were selected to assess *LiDXR* expression across different flowering periods. Total RNA was extracted and reverse-transcribed into cDNA following standard protocols. The qPCR reaction system was prepared according to the manufacturer's instructions for ChamQ Universal SYBR qPCR Master Mix (Vazyme, Nanjing, China), and amplification was carried out under recommended conditions. Each sample included three technical replicates and three biological replicates. Relative gene expression levels were calculated using the $2^{-\Delta\Delta CT}$ method, with $P<0.05$ considered statistically significant. Data were analyzed and visualized using GraphPad Prism 8. The *LrTIP41* gene (GenBank: KJ543466) was used as the internal reference gene. The specific primers for qRT-PCR are listed in Appendix A.

2.6. Subcellular localization

The open reading frame (ORF) of LiDXR was cloned into the pCAMBIA1300-Green fluorescent protein (GFP) vector to generate a fusion protein under the control of the 35S promoter. The resulting fusion vector and the empty GFP vector (control) were separately transformed into *Agrobacterium tumefaciens* GV3101 (Weidi, Shanghai, China). Bacterial cultures were harvested and resuspended in infiltration buffer (10 mmol L^{-1} $MgCl_2$, 100 mmol L^{-1} 2-morpholine ethanesulfonic acid, 200 μmol L^{-1} acetylsyringone, pH 5.8). Transient expression of GFP in tobacco leaves infiltrated with 35S:GFP and 35S:LiDXR-GFP constructs was observed using a Leica TCS SP8 confocal laser scanning microscope (Leica, Germany).

2.7. Virus-induced *LiDXR* gene silencing

For VIGS, two fragments of 250 and 450 bp were selected from positions 288–537 bp and 624–1,073 bp of the *LiDXR* gene sequence and inserted into the TRV2 vector, generating recombinant silencing constructs named TRV2-LiDXR-1 and TRV2-LiDXR-2. These constructs, along with the control TRV1/TRV2 vector, were introduced into *Agrobacterium* strain GV3101. To silence *LiDXR* in *Lilium* petals, 60 'Sorbonne' green buds (at stage S1) were prepared, with peduncles trimmed to 5 cm and randomly assigned to three groups.

During inoculation, the peduncles were immersed in one of three mixed bacterial suspensions: TRV1:TRV2-LiDXR-1 (1:1), TRV1:TRV2-LiDXR-2 (1:1), or TRV1:TRV2 (1:1). Vacuum infiltration was performed at 0.07 kPa for 5 min. After infiltration, the base of each peduncle was rinsed with sterile water, and the buds were placed in vials containing distilled water and subjected to dark treatment for 1 d. Subsequently, buds were transferred to an artificial climate chamber maintained at 20°C until flowering, with water changed daily. Following silencing, the expression of terpene-related genes in 'Sorbonne' was analyzed by qRT-PCR. The specific primers are listed in Appendix A. *LrTIP41* (GenBank: KJ543466) was used as the internal control.

2.8. Transformation and screening of *A. thaliana*

The pBI121-LiDXR vector for stable transformation of *A. thaliana* was constructed similarly to the localization vector, except that it lacked the GFP reporter sequence. The construct was introduced into *A. tumefaciens* GV3101 *via* freeze-thaw transformation. *Arabidopsis thaliana* wild-type (Col-0) plants were transformed by floral dip according to the method described by Willmer *et al.* (2009). Transformed plants were allowed to set seed, and the harvested seeds were sown on Murashige and Skoog (MS) medium supplemented with 20 mg L^{-1} hygromycin B for selection of transformants. Putative transgenic lines were confirmed by RT-PCR, and T_1 and T_2 seeds were collected. T_2 progeny exhibiting hygromycin resistance were advanced to T_3 generation, in which transgenic lines typically showed a segregation ratio consistent with single-locus insertion, and a transformation efficiency of at least 1% was routinely achieved. All transgenic and control plants were grown under a 16 h light/8 h dark photoperiod at 20–22°C.

2.9. Analysis of phenotype and gene expression of *A. thaliana*

To investigate the functional role of *LiDXR* in *A. thaliana*, plant development was divided into four stages: S1 (seedling stage), S2 (green leaf stage), S3 (full flowering stage), and S4 (fruiting stage). Growth status and plant height of four *LiDXR*-transgenic lines, *dxr* mutant, and wild-type plants were recorded across these stages. Growth traits were compared among genotypes, including rosette leaf number, stem length at S2, time to first flowering, and seed yield. At the S2 green leaf stage, chlorophyll *a*, chlorophyll *b*, and carotenoid contents were measured in transgenic, wild-type, and *dxr* mutant plants. The impact of *LiDXR* overexpression on terpenoid biosynthesis and metabolism-related gene expression was analyzed by real-time quantitative PCR. At full flowering, buds with fully exposed white petals were collected from wild-type, *dxr* mutant, and four T_3 transgenic lines (OE-A1, OE-A2, OE-A3, and OE-A4). RNA was extracted and reverse-transcribed into cDNA for qRT-PCR analysis. *AtActin2* (GenBank: AT3G18780) was used as the internal reference gene . The specific primers for qRT-PCR are listed in Appendix A.

2.10. *LiDXR* transformation and identification of petunia

Petunia transformation was performed using the established genetic transformation system for petunia W115. After regeneration, transgenic seedlings capable of normal growth were transplanted into a 1:1 mixture of turf soil and cultivation matrix. Following 3 days of watering and plastic film covering, the film was removed, and plants were maintained under standard growth conditions until flowering and seed set. Genomic DNA was extracted from leaves of transgenic and wild-type petunias using the CTAB method.

2.11. Analysis of phenotype and gene expression of transgenic petunias

To evaluate the effects of *LiDXR* overexpression on petunia growth, the transgenic line exhibiting the highest *LiDXR* expression level was selected for comparison with wild-type plants during the vegetative growth phase. Flower size and corolla tube length were measured at full flowering, and flowering time and duration were recorded. To determine whether *LiDXR* overexpression influenced photosynthetic pigment content, chlorophyll *a*, chlorophyll *b*, and carotenoid levels were quantified in leaves of transgenic and wild-type petunias during vegetative growth. The impact of *LiDXR* overexpression on the expression of terpenoid biosynthesis and metabolism genes was analyzed by real-time quantitative PCR. White petal samples were collected from two T_0 transgenic lines and wild-type plants at full flowering. RNA was extracted and reverse-transcribed into cDNA for qRT-PCR analysis. *PhEF1α* (Mallona *et al.* 2010) was used as the internal reference gene. The specific primers for qRT-PCR are listed in Appendix A.

2.12. Volatile detection and analysis

Volatile organic compounds were analyzed in both silenced and non-silenced 'Sorbonne' flowers. Volatiles were collected using headspace solid-phase microextraction (HS-SPME) and analyzed by gas chromatography-mass spectrometry (GC-MS) on a Shimadzu Nexis GC2030/QP2020NX System (Shimadzu, Japan). Compounds were identified by comparison with the NIST11 database and authentic standards, and emission levels were quantified based on peak areas.

Based on gene expression data, volatile compounds were also analyzed in fully bloomed wild-type petunias and the OE-P2 transgenic line, which exhibited the strongest *LiDXR* overexpression. GC-MS analysis was performed using an Agilent Gas Phase Workstation (Agilent, USA). Mass spectra were matched against the NIST14 database, and compound identities were confirmed using the CAS database.

2.13. Statistical analysis

Data were analyzed using SPSS 20. GraphPad Prism 8, Origin2021, and Photoshop CC were used for data visualization and figure preparation.

3. Results

3.1. Screening of *DXR* gene from the transcriptome of *Lilium* 'Sorbonne'

After removing 27 unigenes corresponding to seven genes in the MEP pathway and standardizing the expression

levels as RPKM, principal component analysis (PCA) was performed on a total of 15 samples, combining five developmental stages and three technical replicates (Fig. 2-B). The first principal component (PC1) accounted for 77.3% of the total variance, and samples from each stage were clearly separated into five distinct clusters. Notably, samples from the pink bud stage (B) and semi-open stage (C) were closely grouped, indicating a high degree of consistency in the expression patterns of the seven MEP pathway genes during these two stages.

Clustering heat map analysis of the standardized RPKM values for the seven MEP pathway genes is shown in Fig. 2-C. All seven genes exhibited a general trend of upregulation followed by downregulation. However, only the *DXR* gene showed a pronounced downregulation at the blooming stage (S4), contrasting sharply with the expression patterns of the other genes. Furthermore, in the terpenoid emission rhythm of *Lilium* flowers, terpenoid release significantly declined from the blooming to the senescence stage. These observations suggest that *DXR* may act as a key rate-limiting gene regulating terpene biosynthesis in the MEP pathway.

3.2. Cloning and characterization of *LiDXR*

The full-length *LiDXR* gene was isolated using RT-PCR. The open reading frame (ORF) of *LiDXR* is 1,419 bp in length and encodes 472 amino acids. The deduced amino acid sequence was compared with DXR sequences from other plant species using NCBI BLASTp. *LiDXR* contains a conserved domain characteristic of the DXR family (Fig. 3-A). All selected plant DXR proteins possess a conserved region of 73–80 amino acids and an N-terminal chloroplast transit peptide. A conserved Cys-Ser-X motif (X=Ala, Val, or Met), which serves as the cleavage site for chloroplast import, was identified in all 11 species, including 'Sorbonne'. Additionally, a Pro-rich motif (PPPAAWP(A)GRA), commonly found in most plants, and the conserved NADPH-binding motif GSTGAIGT, present across all organisms, were detected. Using the LiDXR protein as a query, homologous sequences with over 85% similarity were identified, and a phylogenetic tree was constructed using the neighbor-joining method in MEGA.X. The analysis included monocotyledons, dicotyledons, and algae. 'Sorbonne' LiDXR showed the highest sequence similarity to DzDXR from *Dioscorea zingiberensis* (APW35790.1) (Fig. 3-B). *Dioscorea zingiberensis*, a monocotyledonous species in the *Dioscoreaceae* family, shares the same order (Liliales) as 'Sorbonne', explaining their close phylogenetic relationship.

3.3. Temporal and spatial expression patterns of *LiDXR*

RT-qPCR was used to analyze the expression patterns of *LiDXR* across five flowering stages of 'Sorbonne' and in different tissues — including leaves, petals, anthers, filaments, and pistils — during the half-open stage. The results revealed distinct expression patterns that were consistent with transcriptome data.

The expression level of *LiDXR* varied significantly across

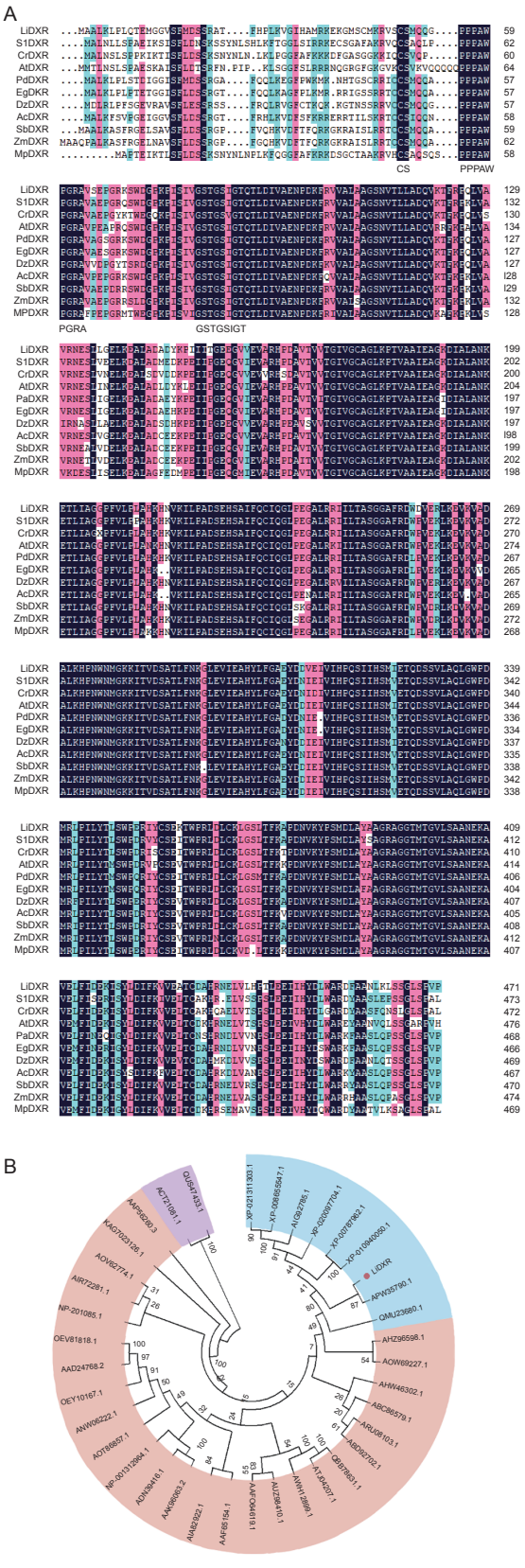


Fig. 3 Phylogenetic analysis and amino acid sequence alignment of LiDXR with homologous proteins. A, multiple sequence alignment of LiDXR and DXR from other plant species. Black, red, and blue shading indicates sequence identity of 100%, ≥75%, and ≥50%, respectively. B, phylogenetic tree of 'Sorbonne' LiDXR and DXR orthologs from diverse species. Blue, monocotyledonous plants; red, dicotyledonous plants; purple, algae.

developmental stages, following a trend of initial increase followed by decrease (Fig. 4-A). Expression increased from the green bud stage to the half-open stage and then declined toward the senescence stage, peaking at the half-open stage. This suggests that *LiDXR* plays a promoting role during early to mid-flowering and may influence floral fragrance formation. Moreover, *LiDXR* expression in floral tissues was significantly higher than in leaves (Fig. 4-B). Specifically, expression in petals was approximately 33-fold higher than in leaves, and in filaments, it was about 15-fold higher. Expression in anthers was relatively low, and significant differences were observed among floral organs. These qRT-PCR results indicate that *LiDXR* is predominantly expressed in petals, which are also the primary site of floral volatile emission in 'Sorbonne'. Thus, *LiDXR* likely plays a crucial role in the biosynthesis and release of floral volatiles.

3.4. Subcellular localization of LiDXR protein

Transgenic tobacco leaf sections were examined under a laser confocal microscope to detect fluorescence signals (Fig. 4-C). The 35S-GFP empty vector was used as a control. Under 488 nm excitation, GFP signals were distributed randomly in the cell membrane, cytoplasm, and nucleus. At approximately 640 nm excitation, chloroplasts exhibited red autofluorescence, and the GFP signal did not overlap with this autofluorescence, confirming proper expression and healthy tissue status. In the experimental group, the green fluorescence signal from the 35S-LiDXR-GFP construct was localized exclusively within chloroplasts. In the merged image, the GFP signal overlapped completely with chloroplast autofluorescence, resulting in a yellow signal. These results confirm that the LiDXR protein from 'Sorbonne' is targeted to chloroplasts, consistent with predictions from subcellular localization software and in agreement with the plastidic localization of the MEP pathway.

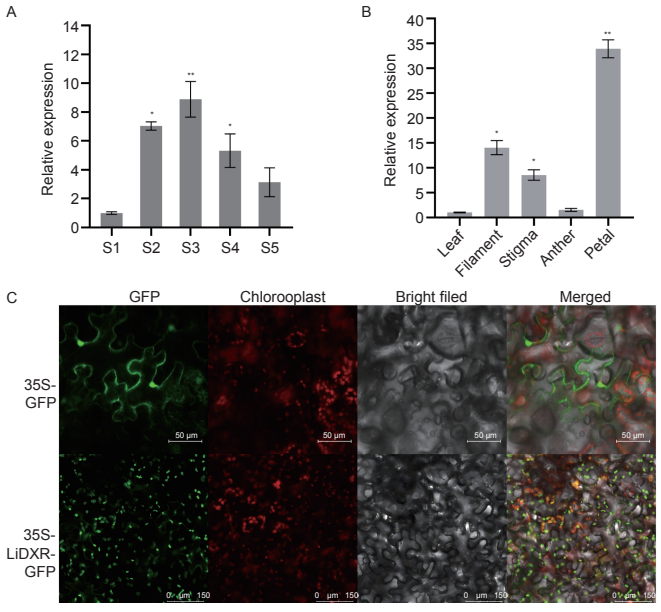


Fig. 4 Expression and subcellular localization analysis of LiDXR. A, temporal expression pattern of *LiDXR* during different developmental stages in 'Sorbonne'. B, tissue-specific expression of *LiDXR* in 'Sorbonne'. The lowest expression level was normalized to 1. Data are presented as mean±SE (n=3). *, P<0.05; **, P<0.01 (two-tailed Student's t-test). C, subcellular localization of LiDXR. The 35S-LiDXR-GFP and 35S-GFP control plasmids were transformed into *Agrobacterium* and infiltrated into tobacco leaves. Scale bars: 50 μm for 35S-GFP; 150 μm for 35S-LiDXR-GFP.

3.5. Expression analysis of terpene-related genes and identification and volatile substances in *LiDXR*-silenced *Lilium* 'Sorbonne'

To determine whether silencing *LiDXR* affects the expression of MEP pathway genes and downstream terpene synthase genes, the expression levels of *LiMCT* and terpene synthase (*TPS*) genes were analyzed. In lily flowers, *TPS1*, *TPS3*, and *TPS4* are responsible for monoterpene synthesis, whereas *TPS2* is involved in sesquiterpene biosynthesis. Analysis of three silenced lily petals revealed that (Fig. 5-A): *LiDXR* silencing efficiency reached approximately 50%, consistent with the typical silencing efficiency of the TRV system. Compared to the empty TRV vector control, the expression of *LiMCT*, a downstream gene in the MEP pathway, was significantly downregulated. Among terpene synthases, the expression levels of the monoterpene synthase genes *TPS1*, *TPS3*, and *TPS4* were significantly reduced in silenced lines, whereas the downregulation of the sesquiterpene synthase *TPS2* was not significant. These results indicate that silencing *LiDXR* in 'Sorbonne' at the pod stage specifically reduces the expression of downstream monoterpene synthase genes in the MEP pathway, thereby decreasing monoterpene biosynthesis and emission.

The major volatile terpenes detected in both silenced and non-silenced lilies included linalool, linalool oxide, and myrcene. The total volatile terpene content in silenced 'Sorbonne' was significantly lower than in controls (Fig. 5-B). This confirms that *LiDXR* silencing disrupts the synthesis of isoprene precursors (IPP and DMAPP), thereby inhibiting downstream terpenoid production in the MEP pathway. However, the precise mechanism of this inhibition requires further investigation.

3.6. Morphological observation of transgenic and mutant *A. thaliana*

Transgenic *A. thaliana*, the *dxr* mutant, and wild-type plants were compared for plant morphology and height at different growth stages (Fig. 6-A). At the S1 seedling stage, all lines except the transgenic OE-A4 strain exhibited similar growth. In the S2 green leaf stage, transgenic lines showed enhanced growth compared to wild-type and mutant plants, although rosette leaf numbers were comparable. At the S3 full flowering stage, transgenic lines maintained their growth advantage, bolting approximately 5 days earlier than wild-type. Wild-type growth gradually caught up, while the mutant displayed clear growth retardation. By the S4 fruiting stage, transgenic lines retained growth and fruiting advantages, producing fruits about 10 days earlier than wild-type. In contrast, the mutant exhibited severe growth stagnation, with no fruiting or defective seed development.

To quantify differences in plant height across stages, data were analyzed for all four developmental phases (Fig. 6-B). Except at the S1 stage, transgenic *A. thaliana* lines showed significantly greater height in the other three stages. Overall, transgenic lines exhibited a clear growth advantage, whereas the *dxr* mutant displayed developmental delays, particularly during reproductive growth.

3.7. Differences in photosynthetic pigments between transgenic and mutant *A. thaliana*

Photosynthetic pigment contents were measured in leaves during the green leaf stage (S2), based on preliminary phenotypic observations (Fig. 6-C). Chlorophyll *a*, chlorophyll *b*, and carotenoid levels in the four transgenic lines were slightly higher than in wild-type, though the differences were modest. In contrast, the *dxr* mutant showed significantly lower levels of all three pigments compared to both wild-type and transgenic lines. These results indicate that mutation of the *dxr* gene in *A. thaliana* impairs photosynthetic pigment accumulation, while overexpression of *LiDXR* has a mild positive effect on chlorophyll and carotenoid content without causing adverse effects.

3.8. Gene expression analysis of transgenic and mutant *A. thaliana* terpenoids

To characterize the MEP pathway, two overexpressing lines (OE-A3 and OE-A4), wild-type, and the *dxr* mutant were selected to analyze the expression of MEP pathway genes *AtMCT* and *AtHDR* in fully bloomed flowers (S3). The expression level of *LiDXR* in the two overexpressing lines was 3.7- and 5.1-fold higher than that of endogenous *AtDXR* in wild-type (Fig. 6-D). Compared to wild-type, *AtDXR* expression was significantly lower in both overexpressing and mutant lines. However, the expression of *AtMCT* and *AtHDR* was significantly upregulated in the overexpressing lines, indicating that *LiDXR* overexpression enhances the expression of downstream MEP pathway genes.

3.9. Phenotype detection of transgenic petunias

Based on semi-quantitative PCR results, petunia lines P1 and P2, which exhibited the highest *LiDXR* overexpression, were selected for phenotypic analysis during vegetative growth (Fig. 7-A) and reproductive development (Fig. 7-B). Compared to the control, P1 and P2 showed larger plant size, longer stems, and enhanced growth vigor during vegetative growth. At full flowering, transgenic petunias bloomed approximately 10 days earlier than wild-type, but no significant differences in leaf or flower morphology were observed. These findings indicate that *LiDXR* transformation in petunia accelerates flowering time and enhances growth potential without altering floral structure.

3.10. Differences in photosynthetic pigments between transgenic and wild petunias

Photosynthetic pigment content was measured in leaves of three transgenic and one wild-type petunia line during vegetative growth (Fig. 7-C). Although leaf morphology appeared similar, transgenic lines exhibited visibly darker green leaves. Quantitatively, chlorophyll *a*, chlorophyll *b*, and carotenoid contents were significantly higher in transgenic lines than in wild-type. These results suggest that *LiDXR* overexpression promotes the synthesis and accumulation of photosynthetic pigments — downstream products of the MEP pathway — resulting in a greener phenotype. However, the impact on petunia floral fragrance remains to be investigated.

3.11. Expression analysis of transgenic petunia terpenoid synthetic genes

The expression levels of MEP pathway and terpenoid biosynthesis genes were analyzed in two overexpressing

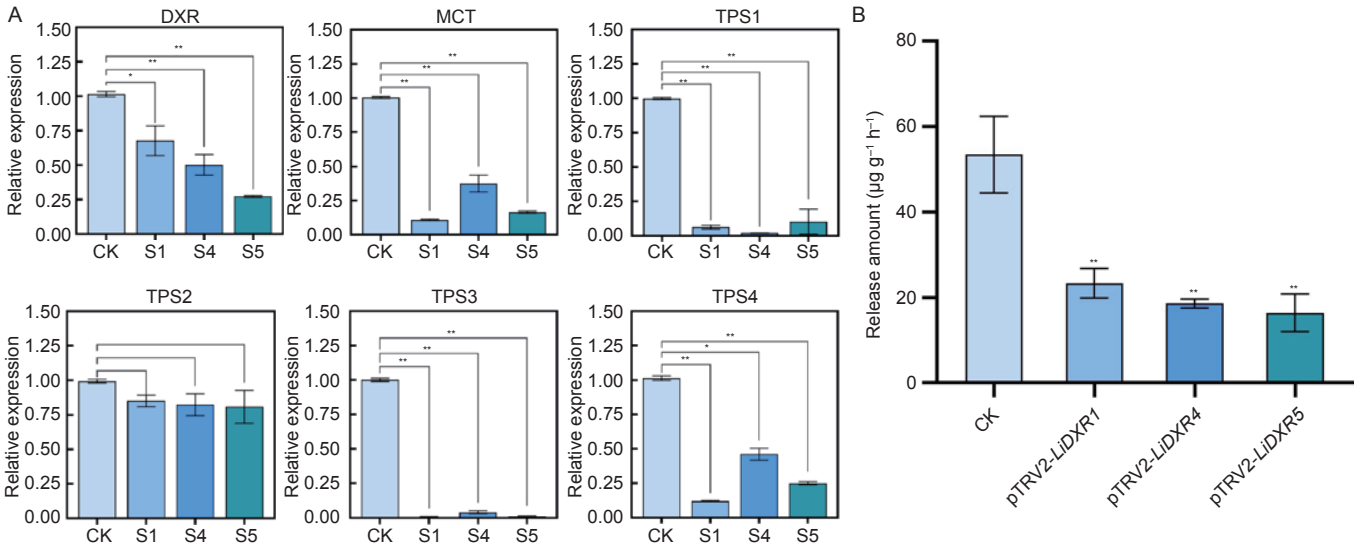


Fig. 5 Analysis of terpene gene and volatile component contents after silencing of *LiDXR* through VIGS technology. A, mixed identification of *LiDXR* silent samples. CK, empty vector control; S1, S4, S5, *LiDXR*-silenced samples. B, volatile component content after *LiDXR* silencing. pTRV2-*LiDXR1*, pTRV2-*LiDXR4*, pTRV2-*LiDXR5*, *LiDXR*-silenced samples. Data are presented as mean±SE (n=3). *, P<0.05; **, P<0.01 (two-tailed Student's t-test).

lines (OE-P1 and OE-P2) and wild-type petunia flowers at the blooming stage. In the overexpressing lines (Fig. 8-A), the expression of the endogenous *PhDXR* gene was significantly reduced, with a more pronounced decrease in OE-P2. In contrast, the expression of *PhMCT* and *PhHDR* was moderately increased.

Since petunia floral terpenes are not well characterized, conserved sequences of the geranyl diphosphate synthase gene (*PhGPPS*) and terpene synthase gene (*PhTPS*) were identified from the petunia genome using homologous BLAST searches, and gene-specific primers were designed to analyze their expression. In the two overexpressing lines (Fig. 8-B), *PhGPPS* expression was 2.4- and 4.2-fold higher than in wild-type, while *PhTPS* expression was approximately 1.6- and 3.5-fold higher, respectively. These findings indicate that the heterologous expression of *LiDXR* in petunia functions similarly to its role in *A. thaliana*, promoting the accumulation of downstream terpenoids and positively influencing plant growth.

3.12. Identification and analysis of volatile substances in transgenic petunia flowers

The results of GC-Murashige and Skoog's (MS) analysis of petunia flowers following mass spectrometry comparison and normalization are presented in Appendix B. The primary volatile compounds in both transgenic and wild-

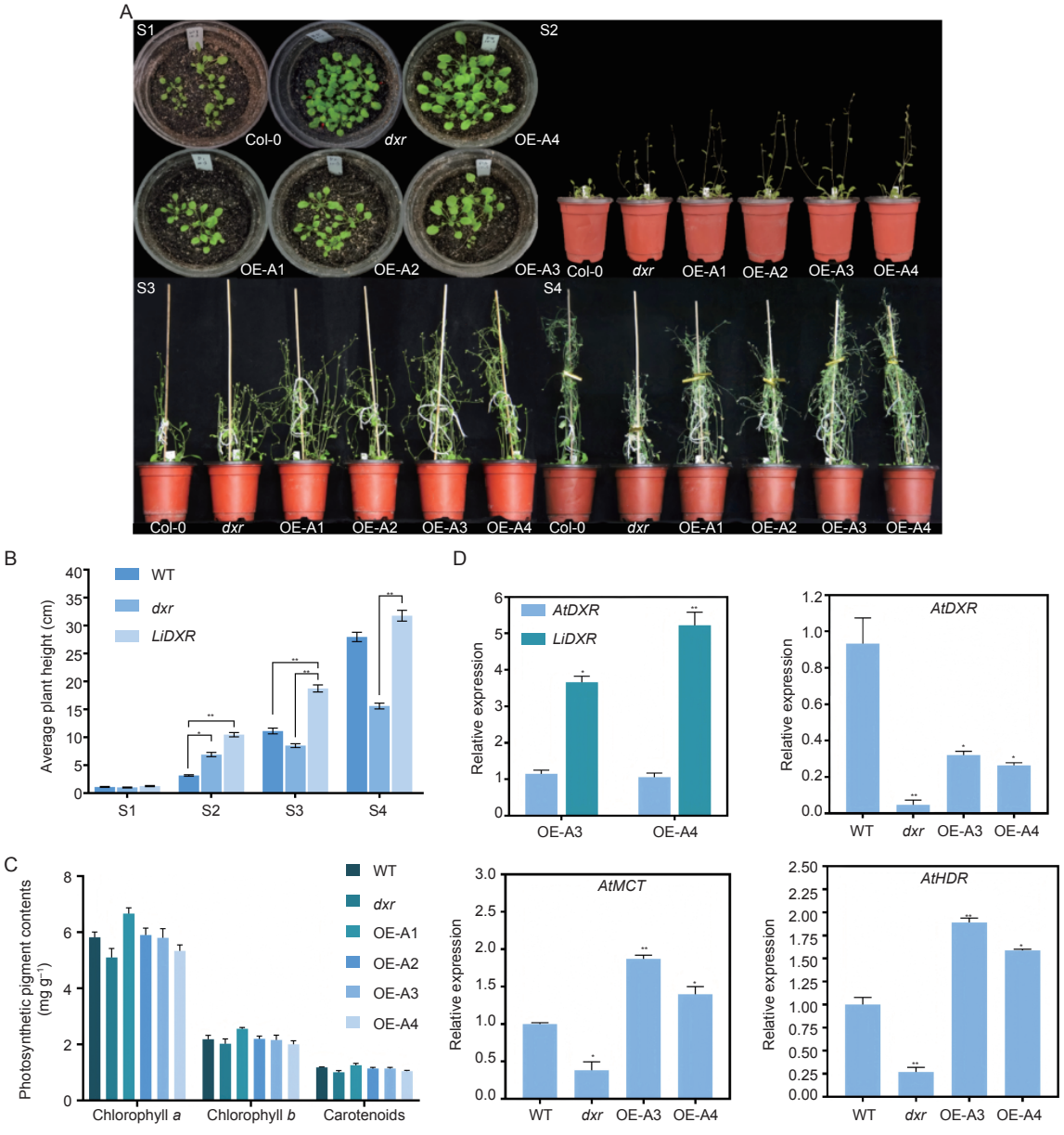


Fig. 6 Phenotypic and molecular characterization of transgenic and mutant *Arabidopsis thaliana*. A, growth comparison of different *A. thaliana* lines across developmental stages. B, plant height ratios of three *A. thaliana* genotypes at different stages. C, photosynthetic pigment content in leaves of different *A. thaliana* lines. D, expression analysis of MEP pathway genes in *A. thaliana*. S1, seedling stage; S2, green leaf stage; S3, full flowering stage; S4, fruiting stage; Col-0 (WT), wild type; *dxr*, mutant; OE-A1, OE-A2, OE-A3, and OE-A4, transgenic *LiDXR* lines. Data are presented as mean±SE (n=3). *, P<0.05; **, P<0.01 (two-tailed Student's t-test).

type petunia flowers at the blooming stage are the aromatic ester methyl benzoate and the phenolic compound *trans*-isoeugenol, with no significant difference in their levels. Together, these compounds account for over 80% of the total volatile content.

The levels of four detected volatile terpenes — sesquiterpene β-ylangene, γ-cadinene, calamenene, and elemene — were significantly higher in transgenic lines compared to wild-type plants. In terms of total volatile terpene content, the mean terpene emission from transgenic petunia lines was approximately 78% greater than that of wild-type (Fig. 8-C). This indicates that overexpression of the *LiDXR* gene in petunia enhances the synthesis of isoprene precursors IPP and DMAPP, thereby promoting the production of downstream terpene metabolites *via* the MEP pathway. Additionally, it redirects a portion of the C5 precursor flux into the MVA pathway, supporting the biosynthesis of sesquiterpenes and other terpenes through cross-talk between the MEP and MVA pathways. However, the precise capacity for C5 precursor exchange requires further experimental design and validation.

4. Discussion

4.1. Expression of *LiDXR* correlates with terpenoid biosynthesis of lily

Floral fragrance is an important ornamental trait in lily. Current studies indicate that terpenes are the primary components of floral volatiles in lily, which are synthesized *via* two distinct pathways in plants: the mevalonate (MVA) pathway in the cytoplasm and the methylerythritol phosphate (MEP) pathway in plastids. The MVA pathway primarily supplies C5 precursors for sesquiterpene and triterpene biosynthesis, whereas the MEP pathway provides C5 precursors for monoterpenes and diterpenes. Exchange of isopentenyl diphosphate (IPP) occurs between these two pathways. Therefore, targeting MEP pathway genes is a rational strategy for enhancing monoterpene biosynthesis in floral tissues. In this study, the MEP pathway gene *LiDXR* was cloned from 'Sorbonne'. The open reading frame (ORF) is 1,419 bp in length. Homologous sequence alignment revealed that the LiDXR protein contains multiple conserved domains and belongs to the DXR superfamily. These sequence features are consistent with previous structural analyses of *AlDXR*, *StDXR*, and *AaDXR* (Xu *et al.* 2023). Phylogenetic analysis showed that LiDXR is most closely related to the DXR protein from *D. zingiberensis*, a monocotyledonous plant, with a bootstrap value of 87, indicating high confidence. This close relationship may reflect the conserved function of DXR proteins, which typically exist as single copies in plants (Guo *et al.* 2022).

4.2. Analysis of *LiDXR* gene expression

The types and quantities of volatile compounds emitted by floral fragrances vary across different tissues and developmental stages of flowers. This variation arises from the differential expression of genes involved in floral volatile biosynthesis, which is regulated by plants in response to developmental cues and environmental conditions. During floral development, the release of aromatic compounds typically peaks when flowers are ready for pollination and

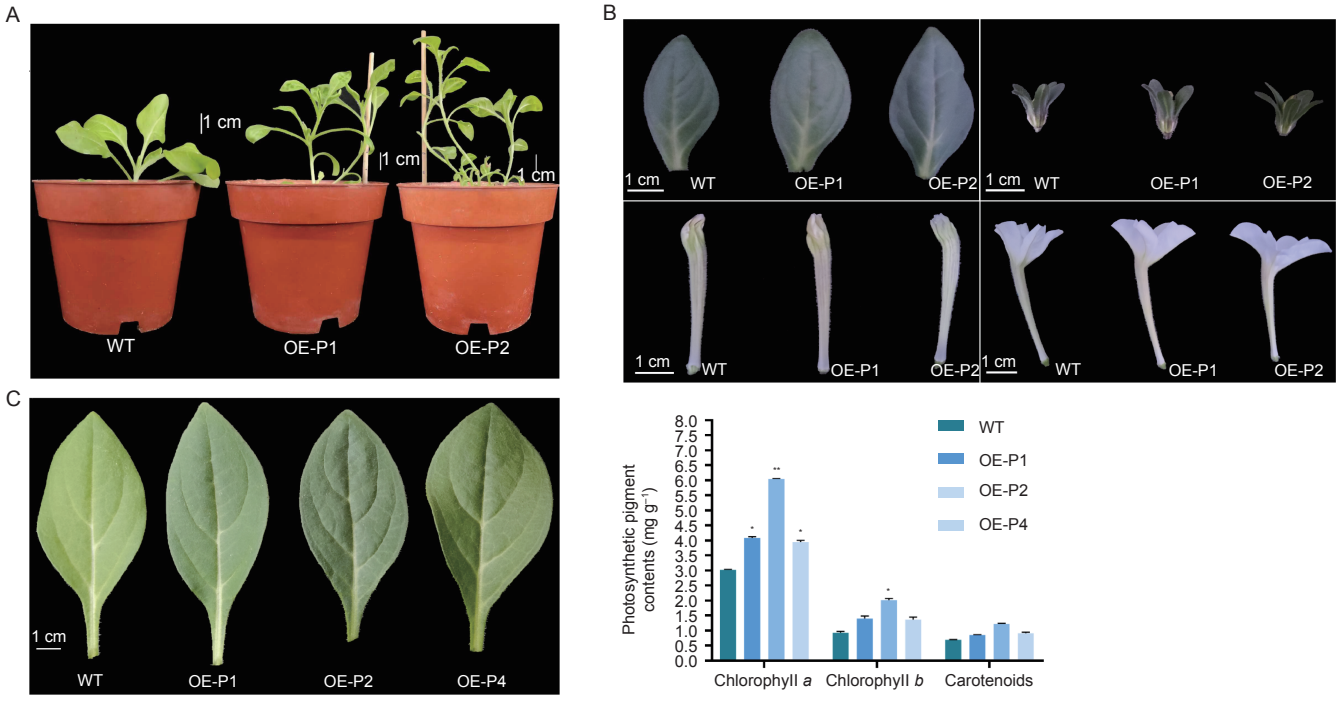


Fig. 7 Phenotypic evaluation of transgenic *Petunia hybrida*. A, comparison of plant architecture and crown diameter. B, morphological comparison of leaves and flowers at full flowering stage. C, photosynthetic pigment content in leaves of transgenic *Petunia hybrida*. WT, wild-type; OE-P1, OE-P2, and OE-P4, transgenic *LiDXR* lines. Data are presented as mean±SE (n=3). *, P<0.05; **, P<0.01 (two-tailed Student's t-test).

then declines rapidly, aligning with the plant's strategy to attract pollinators. Moreover, the expression of biosynthetic genes often precedes volatile emission (Muhlemann *et al.* 2014). In orchids, for example, flowers at the semi-blooming stage are nearly odorless and emit only small amounts of benzene derivatives, whereas fully blooming flowers are strongly fragrant and release substantial quantities of terpenoids, including linalool, primarily from the petal bases. Five monoterpenes — geraniol, β-ocimene, alloocimene, *cis*-citral, and citral — are released exclusively by petals during full bloom (Zheng *et al.* 2023). Our previous study in the laboratory on terpene emissions in 'Sorbonne' demonstrated that volatile terpene release gradually increases from the initial to the full flowering stage and then declines. The relative abundance and diversity of terpenes are the highest during the semi-blooming and blooming stages. The temporal and spatial expression pattern of the *LiDXR* gene closely mirrors the dynamics of terpene emission in lily, consistent with findings in other flowering species. This suggests that *LiDXR* expression is closely associated with the regulation of terpene biosynthesis and release in 'Sorbonne'.

Consistent with the regulatory patterns of floral volatile biosynthesis, *TPS* genes, which encode terpene synthases, often reach peak expression 1–2 days before the corresponding volatiles are released, and their expression declines during petal senescence. In roses, certain *RcTPS* genes exhibit peak expression in flowers or floral buds, correlating with terpenoid synthesis and emission profiles in petals (Kong *et al.* 2022). Volatile emission also displays marked tissue specificity. As a key rate-limiting enzyme-encoding gene in the MEP pathway, *LiDXR* may directly influence terpene content through its expression level. During the half-opening stage, *LiDXR* expression in different floral organs of 'Sorbonne' was tissue-specific, with significantly higher levels in petals than in other floral parts. In plum blossoms, GC-MS analysis revealed that over 90% of volatile compounds are released by petals. Similarly, the study on clematis flowers support the conclusion that petals are the primary site of floral fragrance emission (Jiang *et al.* 2020). The tissue-specific expression pattern of *LiDXR* observed in this study aligns with findings in other species, indicating that *LiDXR* plays a significant role in the biosynthesis of floral volatiles in lily petals.

4.3. Subcellular localization and functional verification

Plant somatic cells possess a complex subcellular architecture, and the correct localization of proteins is essential for their biological function and cellular activity. Subcellular localization is a critical technique in gene functional analysis, providing key insights into the progression from gene expression to protein function. The protein encoded by the *DXR* gene typically contains a plastid transit peptide, supporting its localization to plastids. Studies have confirmed that MEP pathway enzymes are predominantly localized in plastids. Subcellular localization analyses in species such as *Liriodendron* and maize have demonstrated that DXR proteins function in chloroplasts (Hans *et al.* 2004; Zhang *et al.* 2022). In this study, transient expression of a fluorescent fusion vector in tobacco leaves confirmed that

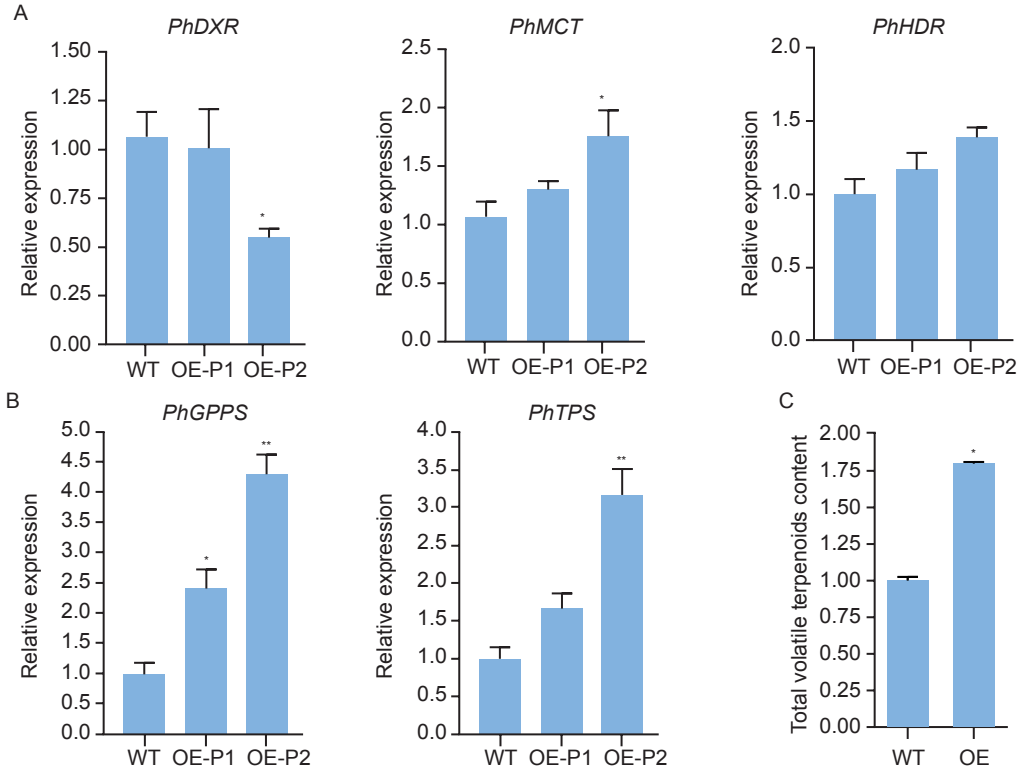


Fig. 8 Analysis of terpenoid biosynthesis genes and floral volatiles in transgenic petunias. A, expression of MEP pathway genes in *Petunia hybrida*. B, expression of terpene synthase genes in *P. hybrida*. C, comparison of total volatile terpenoid content between transgenic and wild-type *P. hybrida*. Data are presented as mean±SE (n=3). *, P<0.05; **, P<0.01 (two-tailed Student's t-test).

LiDXR protein localizes to plastid chloroplasts. This result is consistent with findings in *A. thaliana*, where MEP pathway genes are localized and function within plastids (Pokhilko *et al.* 2015). Given the functional role of chloroplasts, the MEP pathway not only supplies C5 precursors for volatile terpene biosynthesis but also contributes to the synthesis of photosynthetic pigments such as chlorophyll, offering additional avenues for functional validation of DXR.

DXR is a key rate-limiting enzyme in the plant MEP pathway. Alterations in *DXR* expression — whether through overexpression or suppression — directly affect the production of MEP-derived metabolites and can influence plant phenotypes. In this study, the *LiDXR* gene in 'Sorbonne' was silenced using a VIGS system. Compared to controls, the expression of MEP pathway genes and monoterpene synthase genes was significantly reduced. In *A. thaliana dxr* mutants, complete disruption of the MEP pathway results in leaf chlorosis, a phenotype indicative of carotenoid deficiency, along with abnormal chloroplast and trichome development and stunted growth, likely due to deficiencies in gibberellin and abscisic acid precursors (Xing *et al.* 2010). The *A. thaliana dxr* mutant used in this study exhibited similar leaf yellowing and growth retardation. Similarly, VIGS-mediated silencing of *DXR* in mulberry led to wrinkled leaves and significantly reduced levels of chlorophyll *b* and total chlorophyll compared to control plants (Li *et al.* 2022). These phenotypes observed in *DXR*-silenced or mutant plants suggest that disruption of the plastidic MEP pathway leads to insufficient biosynthesis of photosynthetic pigments, gibberellins, and abscisic acid. The C5 flux from the cytosolic MVA pathway is insufficient to compensate for the deficit in the plastidic MEP pathway, resulting in developmental abnormalities. These findings underscore the essential role of *DXR* in regulating isoprenoid biosynthesis.

Conversely, in transgenic *A. thaliana* and petunia plants transformed with the plant expression vector pBI121-LiDXR, overexpression of *LiDXR* promoted plant growth and development, with transgenic lines exhibiting superior growth potential and increased leaf photosynthetic pigment content compared to wild-type plants. In *A. thaliana* overexpressing DXR, carotenoid and photosynthetic pigment levels were significantly elevated, along with enhanced *DXR* enzyme activity and increased plant height (Carretero-Paulet *et al.* 2006). Overexpression of *NtDXR1* in tobacco up-regulated transcripts of other MEP pathway genes, leading to increased levels of photosynthetic pigments, leaf surface volatile essential oils, and hormones *via* the MEP pathway (Zhang *et al.* 2015). These results suggest that *DXR* overexpression enhances chlorophyll content, thereby improving photosynthetic capacity and nutrient accumulation to support plant growth. Regarding terpene characterization, the expression of downstream genes in transgenic plants, particularly those encoding monoterpene synthases, was significantly up-regulated. In peppermint, overexpression of *DXR* increased the synthesis and release of terpene essential oils without altering the terpene profile (Mahmoud and Croteau 2001), a result consistent with our findings. Interestingly, in transgenic plants overexpressing *LiDXR*, the expression of endogenous *DXR* genes — including *AtDXR* and *PhDXR* — was significantly suppressed, with expression levels reduced to approximately half of those in controls, suggesting the involvement of a negative feedback regulatory mechanism.

Combining the phenotypic observations from transgenic *A. thaliana*, *dxr* mutants, and transgenic petunias, it is evident that overexpression of *LiDXR* plays a pivotal role in directing metabolic flux toward the biosynthesis of IPP and DMAPP. The accumulation of DXR protein in transgenic plants enhances the "push" effect on the downstream pool of C5 precursors, leading to increased production of geranyl diphosphate (GPP) and geranylgeranyl diphosphate (GGPP) — precursors for monoterpenes and diterpenes, respectively — and ultimately resulting in elevated synthesis and emission of end products, including monoterpenes, *via* the MEP pathway.

5. Conclusion

In this study, the *LiDXR* gene of the MEP pathway was cloned from *Lilium* 'Sorbonne'. Its expression level peaked at the half-opening stage of flowers and was significantly higher in petals than in other floral organs. Silencing of the *LiDXR* gene suppressed the expression of MEP pathway genes and downstream monoterpene synthase genes, thereby inhibiting the biosynthesis of floral volatile monoterpenes. Overexpression of *LiDXR* in the model plant *A. thaliana* and the ornamental plant *P. hybrida* not only enhanced the biosynthesis of floral terpenoids, but also increased the accumulation of MEP pathway products, including photosynthetic pigments, promoted plant growth vigor, and accelerated flowering time.

Acknowledgements

This research was supported by the Key Research and Development Program of the Ministry of Science and Technology, China (2016YFC0500306-02) and the Project of the Science and Technology Department of Heilongjiang Province, China (C2017030).

Declaration of competing interest

The authors declare that they have no conflict of interest.

Declaration of generative AI and AI-assisted technologies in the writing process

The authors declare that they did not use AI in the preparation and writing of this manuscript.

Appendices associated with this paper are available at https://doi.org/10.1016/j.jia.2025.11.002

References

Carretero-Paulet L, Ahumada I, Cunillera N, Rodriguez-Concepcion M, Ferrer A, Boronat A, Campos N. 2002. Expression and molecular analysis of the *Arabidopsis DXR* gene encoding 1-deoxy-D-xylulose 5-phosphate reductoisomerase, the first committed enzyme of the 2-C-methyl-D-erythritol 4-phosphate pathway. *Plant Physiology*, **129**, 1581–1591.

Carretero-Paulet L, Cairo A, Botella-Pavia P, Besumbes O, Campos N, Boronat A, Rodriguez-Concepcion M. 2006. Enhanced flux through the methylerythritol 4-phosphate pathway in *Arabidopsis* plants

overexpressing deoxyxylulose 5-phosphate reductoisomerase. *Plant Molecular Biology*, **62**, 683–695.
Guo X, Li Q, Yan B, Wang Y, Wang S, Xiong F, Zhang C, Zhang Y, Guo L. 2022. Mild shading promotes sesquiterpenoid synthesis and accumulation in *Atractylodes lancea* by regulating photosynthesis and phytohormones. *Scientific Reports*, **121**, 21648.
Hans J, Hause B, Strack D, Walter M H. 2004. Cloning, characterization, and immunolocalization of a mycorrhiza-inducible 1-deoxy-d-xylulose 5-phosphate reductoisomerase in arbuscule-containing cells of maize. *Plant Physiology*, **134**, 614–624.
Jadaun J S, Sangwan N S, Narnoliya L K, Singh N, Bansal S, Mishra B, Sangwan R S. 2017. Over-expression of *DXS* gene enhances terpenoidal secondary metabolite accumulation in rose-scented geranium and *Withania somnifera*: Active involvement of plastid isoprenogenic pathway in their biosynthesis. *Physiologia Plantarum*, **159**, 381–400.
Jiang Y, Qian R, Zhang W, Wei G, Ma X, Zheng J, Kollner T G, Chen F. 2020. Composition and biosynthesis of scent compounds from sterile flowers of an ornamental plant *Clematis florida* cv. 'Kaiser'. *Molecules*, **25**, 1711.
Johnson T S, Schwieterman M L, Kim J Y, Cho K H, Clark D G, Colquhoun T A. 2016. *Lilium* floral fragrance: A biochemical and genetic resource for aroma and flavor. *Phytochemistry*, **122**, 103–112.
Kong Y, Sun M, Pan H, Zhang Q. 2012. Composition and emission rhythm of floral scent volatiles from eight lily cut flowers. *Journal of the American Society for Horticultural Science*, **137**, 376–382.
Kong Y, Wang H, Lang L, Dou X, Bai J. 2022. Effect of developmental stages on genes involved in middle and downstream pathway of volatile terpene biosynthesis in rose petals. *Genes*, **137**, 26–65.
Li Y, Yu C, Mo R, Zhu Z, Dong Z, Hu X, Deng W, Zhuang C. 2022. Screening and verification of photosynthesis and chloroplast-related genes in mulberry by comparative RNA-Seq and virus-induced gene silencing. *International Journal of Molecular Sciences*, **23**, 8620.
Mahmoud S S, Croteau R B. 2001. Metabolic engineering of essential oil yield and composition in mint by altering expression of deoxyxylulose phosphate reductoisomerase and menthofuran synthase. *Proceedings of the National Academy of Sciences of the United States of America*, **98**, 8915–8920.
Mallona I, Lischewski S, Weiss J, Hause B, Egea-Cortines M J B P B. 2010. Validation of reference genes for quantitative real-time PCR during leaf and flower development in *Petunia hybrida*. *BMC Plant Biology*, **10**, 4.
Muhlemann J K, Klempien A, Dudareva N. 2014. Floral volatiles: From biosynthesis to function. *Plant*, *Cell & Environment*, **37**, 1936–1949.
Opitz S, Nes W D, Gershenzon J. 2014. Both methylerythritol phosphate and mevalonate pathways contribute to biosynthesis of each of the major isoprenoid classes in young cotton seedlings. *Phytochemistry*, **98**, 110–119.
Orru A, Marchese G, Ruiu S. 2023. Alkaloids in *Withania somnifera* (L.) dunal root extract contribute to its anti-inflammatory activity. *Pharmacology*, **108**, 301–307.
Pichersky E, Noel J P, Dudareva N. 2006. Biosynthesis of plant volatiles: Nature's diversity and ingenuity. *Science*, **311**, 808–811.
Pokhilko A, Bou-Torrent J, Pulido P, Rodriguez-Concepcion M, Ebenhoh O. 2015. Mathematical modelling of the diurnal regulation of the MEP pathway in *Arabidopsis*. *The New Phytologist*, **206**, 1075–1085.
Tholl D, Chen F, Petri J, Gershenzon J, Pichersky E. 2005. Two sesquiterpene synthases are responsible for the complex mixture of sesquiterpenes emitted from Arabidopsis flowers. *The Plant Journal*, **42**, 757–771.
Willmer P G, Nuttman C V, Raine N E, Stone G N, Knudsen J T. 2009. Floral volatiles controlling ant behaviour. *Functional Ecology*, **23**, 888–900.
Xing S, Miao J, Li S, Qin G, Tang S, Li H, Gu H, Qu L J. 2010. Disruption of the 1-deoxy-D-xylulose-5-phosphate reductoisomerase (*DXR*) gene results in albino, dwarf and defects in trichome initiation and stomata closure in *Arabidopsis*. *Cell Research*, **20**, 688–700.
Xu R, Wu J, Zhang Y, Jiang L, Yao J, Zha L, Xie J. 2023. Isolation, characterisation, and expression profiling of *DXS* and *DXR* genes in *Atractylodes lancea*. *Genome*, **66**, 150–164.
Yao H, Gong Y, Zuo K, Ling H, Qiu C, Zhang F, Wang Y, Pi Y, Liu X, Sun X, Tang K. 2008. Molecular cloning, expression profiling and functional analysis of a *DXR* gene encoding 1-deoxy-D-xylulose 5-phosphate reductoisomerase from *Camptotheca acuminata*. *Journal of Plant Physiology*, **165**, 203–213.
Zhang C, Liu H, Hu S, Zong Y, Xia H, Li H. 2022. Transcriptomic profiling of the floral fragrance biosynthesis pathway of *Liriodendron* and functional characterization of the *LtuDXR* gene. *Plant Science*, **314**, 111124.
Zhang H, Niu D, Wang J, Zhang S, Yang Y, Jia H, Cui H. 2015. Engineering a platform for photosynthetic pigment, hormone and cembrane-related diterpenoid production in *Nicotiana tabacum*. *Plant & Cell Physiology*, **56**, 2125–2138.
Zheng B Q, Li X Q, Wang Y. 2023. New insights into the mechanism of spatiotemporal scent accumulation in orchid flowers. *Plants*, **12**, 304.

Executive Editor-in-Chief Sanwen Huang
Managing Editor Lingyun Weng